

The Pion Form Factor from Lattic QCD \diamond

Ph. Hägler and in collaboration with QCDSF/UKQCD (D. Brömmel et al.)

The lightest QCD bound state, the pion, plays a central role in chiral symmetry breaking and for the low-energy dynamics of QCD, and a thorough investigation of its internal structure in terms of quark and gluon degrees of freedom is particularly interesting. For some time now it has been possible to explore the structure of hadrons from first principles using lattice QCD, and in 2005 we have started to investigate the structure of the pion in the framework of generalised parton distributions [1], which contain both parton distributions and form factors as limiting cases. Here we report on our recent detailed analysis [2] of the pion electromagnetic form factor F_π from $N_f = 2$ lattice QCD simulations, based on $O(a)$ improved Wilson fermions and Wilson glue. We improve upon recent simulations in quenched [3] and unquenched QCD [4] by extracting the pion form factor for a large number of coupling (β) and quark mass (κ) combinations, which allows us to study both the chiral and the continuum limit. The pion electromagnetic form factor F_π describes the coupling of the vector current to the pion and is defined by $\langle \pi^+(p') | V_\mu(0) | \pi^+(p) \rangle = (p'_\mu + p_\mu) F_\pi(Q^2)$ where the momentum transfer is $q_\mu = (p'_\mu - p_\mu)$, and $q^2 = -Q^2$. Due to isospin symmetry, the vector current can be rewritten to contain only a single flavour, e.g. $V_\mu = \bar{u}\gamma_\mu u$. In the lattice simulation, we have used the unimproved local vector current, and our analysis shows that corrections due to the improvement term [5] are quite small. Since the corresponding lattice current is not conserved, it has to be renormalized by demanding that $F_\pi(Q^2 = 0) = 1$. The computation of the pion matrix element on the lattice follows a standard procedure based on an appropriate ratio of lattice three- and two-point-functions [6].

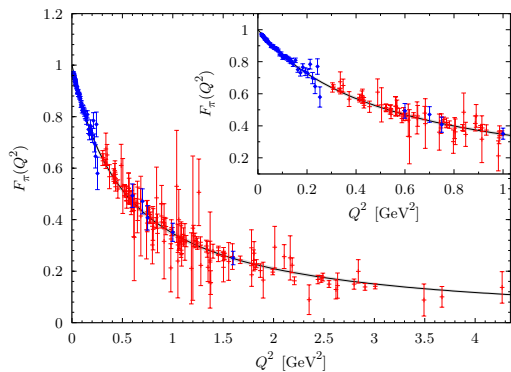


Figure 1: Combined results for the pion form factor for all pion masses and lattice spacings together with a global fit. Experimental data is represented by blue diamonds.

We find that the pion form factor is described very well by a monopole form for the full range of available lattice pion masses. Assuming a linear dependence of the monopole mass squared on the pion mass squared, $M_{mono}^2 = c_0 + c_1 m_\pi^2$, we performed a combined fit to all our lattice data. Figure 1 shows the experimental data for

$F_\pi(Q^2)$ along with the result of the combined fit F_π^{fit} . For this plot, the lattice data at different lattice pion masses has been shifted to the physical pion mass and plotted on-top of the extrapolation. This has been achieved by subtracting the difference $F_\pi^{fit}(Q^2, m_{\pi,lat}^2) - F_\pi^{fit}(Q^2, m_{\pi,phys}^2)$ from the individual lattice points. The excellent agreement between our simulation and the experimental results is emphasised by the insert in Fig. 1, which shows the region $Q^2 < 1\text{GeV}^2$, where most of the experimental points lie.

In addition, we performed monopole fits to all individual datasets at fixed pion masses to obtain M_{mono}^2 as a function of the pion mass. A linear chiral extrapolation to the physical pion mass is shown in Fig. 2. This leads to our final result of $M_{mono}(m_{\pi,phys}) = 0.729(16)\text{GeV}$ for the monopole mass. The large set of β, κ -values we used allowed us to study possible lattice artifacts arising from the finite lattice spacing and volume. An empirical fit including a volume dependence leads to a small increase of the monopole mass by 3% at infinite volume. Furthermore, we find no significant dependence on the lattice spacing within errors, in the range $a = 0.07 - 0.11\text{ fm}$ of our simulations. Our result for the monopole mass corresponds to a charge radius squared of $\langle r^2 \rangle = 0.440(19)\text{fm}^2$ at the physical point, in very good agreement with experiment, $\langle r^2 \rangle = 0.452(11)\text{fm}^2$ (see Particle Data Group 2004).

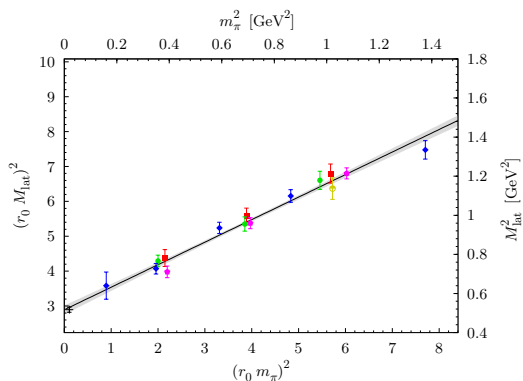


Figure 2: Linear chiral extrapolation of the monopole mass to the physical point.

References

- [1] D. Brömmel *et al.* [QCDSF/UKQCD], Proc. Sci. **LAT2005** (2005) 360
- [2] D. Brömmel *et al.* [QCDSF/UKQCD], arXiv:hep-lat/0608021.
- [3] BGR Collaboration, S. Capitani *et al.*, Phys. Rev. **D73** (2006) 034505
J. van der Heide *et al.*, Phys. Rev. **D69** (2004) 094511
A.M. Abdel-Rehim and R. Lewis, Phys. Rev. **D71** (2005) 014503
RBC Collaboration, Y. Nemoto, Nucl. Phys. Proc. Suppl. **129** (2004) 299
- [4] LHP Collaboration, F. D. R. Bonnet *et al.*, Phys. Rev. **D72** (2005) 054506
JLQCD Collaboration, S. Hashimoto *et al.* PoS **LAT2005** (2006) 336
- [5] S. Sint and P. Weisz, Nucl. Phys. **B502** (1997) 251
- [6] M. Göckeler *et al.*, [QCDSF], Phys. Rev. **D71** (2005) 034508

\diamond Supported by the DFG Emmy-Noether-Program, the EU Integrated Infrastructure Initiative “Hadron Physics” (I3HP) and the Helmholtz Association.